Article

Elucidating the Vibrational Spectra of Hydrogen-Bonded Aggregates in Solution: Electronic Structure Calculations with Implicit Solvent and First-Principles Molecular Dynamics Simulations with Explicit Solvent for 1-Hexanol in *n*-Hexane

John M. Stubbs, and J. Ilja Siepmann

J. Am. Chem. Soc., **2005**, 127 (13), 4722-4729• DOI: 10.1021/ja044380q • Publication Date (Web): 12 March 2005

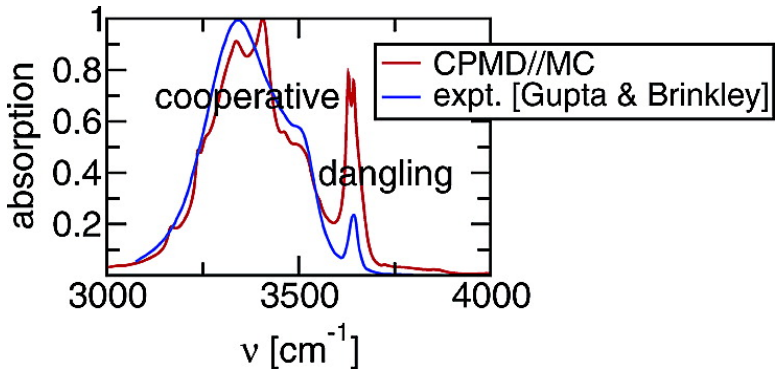

More About This Article

Additional resources and features associated with this article are available within the HTML version:

- Supporting Information
- Links to the 2 articles that cite this article, as of the time of this article download
- Access to high resolution figures
- Links to articles and content related to this article
- Copyright permission to reproduce figures and/or text from this article

View the Full Text HTML

J|A|C|S
ARTICLES
Published on Web 03/12/2005

Elucidating the Vibrational Spectra of Hydrogen-Bonded Aggregates in Solution: Electronic Structure Calculations with Implicit Solvent and First-Principles Molecular Dynamics Simulations with Explicit Solvent for 1-Hexanol in *n*-Hexane

John M. Stubbs† and J. Ilja Siepmann*

Contribution from the Departments of Chemistry and Chemical Engineering and Materials Science, University of Minnesota, 207 Pleasant Street SE, Minneapolis, Minnesota 55455-0431, and Chemistry and Materials Science Directorate, Lawrence Livermore National Laboratory, Livermore, California 94550

Received September 15, 2004; E-mail: siepmann@chem.umn.edu

Abstract: Fourier transform infrared spectroscopy is a popular method for the experimental investigation of hydrogen-bonded aggregates, but linking spectral information to microscopic information on aggregate size distribution and aggregate architecture is an arduous task. Static electronic structure calculations with an implicit solvent model, Car−Parrinello molecular dynamics (CPMD) using the Becke−Lee−Yang−Parr (BLYP) exchange and correlation energy functionals and classical molecular dynamics simulations for the all-atom version of the optimized parameters for liquid simulations (OPLS-AA) force field were carried out for an ensemble of 1-hexanol aggregates solvated in *n*-hexane. The initial configurations for these calculations were size-selected from a distribution of aggregates obtained from a large-scale Monte Carlo simulation. The vibrational spectra computed from the static electronic structure calculations for monomers and dimers and from the CPMD simulations for aggregates up to pentamers demonstrate the extent of the contribution of dangling or nondonating hydroxyl groups found in linear and branched aggregates to the "monomeric" peak. Furthermore, the computed spectra show that there is no simple relationship between peak shift and aggregate size nor architecture, but the effect of hydrogen-bond cooperativity is shown to differentiate polymer-like (cooperative) and dimer-like (noncooperative) hydrogen bonds in the vibrational spectrum. In contrast to the static electronic structure calculations and the CPMD simulations, the classical molecular dynamics simulations greatly underestimate the vibrational peak shift due to hydrogen bonding.

I. Introduction

The hydrogen-bonding interaction is a strong and directional interaction that dominates the association of many molecules. Alcohols, having a hydroxyl headgroup attached to an organic tail, associate in both neat liquids and solutions with a variety of molecular aggregates formed based on molecular structure and thermodynamic state point (temperature, pressure, and composition). Alcohol aggregates in dilute nonpolar solutions have found direct technological application due to their beneficial impact on the properties of the solution, such as enhancing a supercritical fluid's solvating power or solubilizing water contamination in fuel mixtures, and have been the subject of many experimental investigations.[1−4] The extent of hydrogen bonding in alcohol aggregates can be conveniently probed through nuclear magnetic resonance (NMR) or Fourier transform infrared spectroscopy (FT-IR). In the latter case, a hydroxyl group participating as the donor in a hydrogen bond has a shifted vibrational frequency appearing as a broad band centered at 3350 cm^{-1} as compared to a non-hydrogen-bonding hydrogen with a vibrational frequency of ∼3650 cm^{-1}.[4] With the fraction of donating hydroxyl groups known through these quantitative spectral measures, various models can be employed to analyze the results, the most prevalent being an assumption of an equilibrium between monomers and cyclic tetramer structures.[1−3,5,6] It is known, however, that a situation where a given hydroxyl group is acting as a hydrogen-bond acceptor but not donor will result in this hydroxyl group appearing as isolated with respect to spectroscopic probing.[2,7−11] This can lead to an overestimation of the concentration of "isolated" molecules. In the extreme case, a dimeric structure of two alcohols is thought to only form a single hydrogen bond, so that every dimer spuriously contributes one count to the isolated molecule

† Present address: Department of Chemistry, Grinnell College, 1116 8th Avenue, Grinnell, IA 50112.

(1) Fulton, J. L.; Yee, G. G.; Smith, R. D. *J. Am. Chem. Soc.* **1991**, *113*, 8327.
(2) Karachewski, A. M.; Howell, W. J.; Eckert, C. A. *AIChE J.* **1992**, *37*, 65.
(3) Taylor, C. M. V.; Bai, S.; Mayne, C. L.; Grant, D. M. *J. Phys. Chem. B* **1997**, *101*, 5652.
(4) Gupta, R. B.; Brinkley, R. L. *AIChE J.* **1998**, *44*, 207.
(5) Curtiss, L. A. *J. Chem. Phys.* **1977**, *67*, 1144.
(6) Czeslik, C.; Jonas, J. *Chem. Phys. Lett.* **1999**, *302*, 633.
(7) Luck, W. A. P.; Schrems, O. *J. Mol. Struct.* **1980**, *60*, 333.
(8) Yamaguchi, Y.; Yasutake, N.; Nagaoka, M. *J. Phys. Chem. A* **2002**, *106*, 404.
(9) Mó, O.; Yáñez, M.; Elguero, J. *J. Mol. Struct. (THEOCHEM)* **1994**, *314*, 73.
(10) Hagemeister, F. C.; Gruenloh, C. J.; Zwier, T. S. *J. Phys. Chem. A* **1998**, *102*, 82.
(11) Schall, H.; Häber, T.; Suhm, M. A. *J. Phys. Chem. A* **2000**, *104*, 265.

10.1021/ja044380q CCC: $30.25

measure. In contrast, all hydroxyl groups in a cyclic structure act as donors. Thus, in a system that contains only isolated molecules (acting as neither donor nor acceptor) and cyclic aggregates, the number of free donors is equal to the number of isolated molecules.

Additionally, it might be possible to deconvolute the hydrogen-bonded vibrational spectral peak into multiple peaks assumed to arise from varying aggregate sizes.[4] The problem of correlating a spectrum to a distribution over structural motifs then becomes one of knowing, on average, how many free or "dangling" hydroxyl groups are present for a specific structural motif. Hydrogen-bond cooperativity is known[4,9−15] to enhance the stability of hydrogen bonds formed with acceptors that are already participating in a hydrogen bond. Conversely, hydrogen bonds formed without the influence of the cooperative effect should be comparatively less stable and hence appear with a smaller spectral shift with respect to the isolated vibrational peak that has been the subject of several experimental[7,12,13,16] and computational studies.[9,10,17] For the system of methanol in argon matrixes, experimental peak shifts of -140 and -300 cm^{-1} were found for dimer-like (no cooperative effect) and for polymer-like hydrogen bonds.[7] An experimental gas-phase study of methanol[16] found the peak shift due to dimer formation to be -107 cm^{-1}. Peak shifts of -107 and $+3$ cm^{-1} for the donating and accepting hydroxyl groups of the linear dimer were observed in a more recent high-resolution study of low-temperature gas-phase methanol clusters using cavity ringdown laser absorption spectroscopy (CRLAS).[12] In addition, this CRLAS study yielded larger red shifts of -210 and -400 cm^{-1} for the main spectral peaks of the cyclic trimer and tetramer. Furthermore, in another CRLAS investigation for 1-butanol[13] slightly larger magnitudes of the shifts were measured for the dimers (-140 cm^{-1}), trimers (-230 cm^{-1}), and tetramers (-400 cm^{-1}), as an increase in the length of the alkyl tail results in an increase in the hydrogen-bond strength. Finally, even at low temperatures the spectral features for 1-butanol are significantly broadened compared to methanol because of the many conformational states of the longer side chains.[12,13]

A snapshot taken from a previous large-scale Monte Carlo (MC) simulation for a 3% solution of 1-hexanol in *n*-hexane[18] is shown in Figure 1 and clearly reveals the tendency of the 1-hexanol molecules to aggregate. These calculations made use of identity switch moves[19] to efficiently sample the spatial distribution of the 1-hexanol molecules and were carried out for systems using a total of 1000 molecules and the united-atom version of the transferable potentials for phase equilibria (TraPPE-UA) force field.[20,21] A structural analysis of these large-scale simulations demonstrated the existence of a variety of hydrogen-bonded aggregates with a preference for tetrameric and pentameric aggregates (see Figure 2). Beyond trimers, aggregates of the same size are found to have multiple preferable architectures. For this system, a comparison to the FT-IR experimental data[4] showed good agreement for the fraction of hydroxyl groups determined from the "monomeric" spectral peak and the fraction of nondonating hydroxyl groups observed in the simulations. In contrast, the calculated fraction of true monomers that neither accept nor donate a hydrogen bond was found to be substantially smaller by as much as 50%.[18]

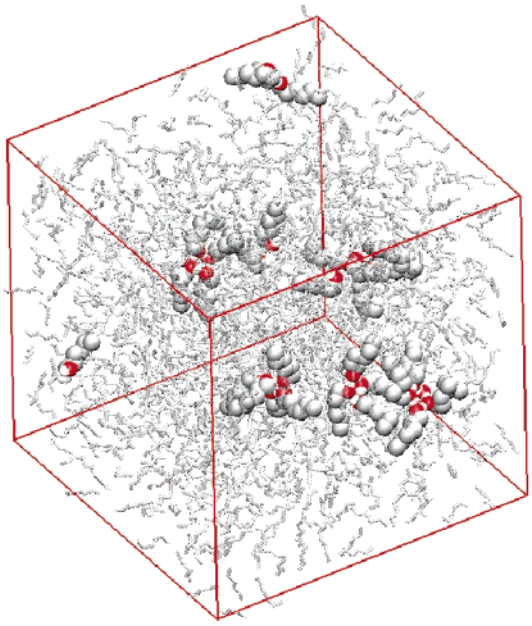

Figure 1. Snapshot taken from a large-scale Monte Carlo simulation[18] of a 3% solution of 1-hexanol in *n*-hexane at $T = 298$ K and $p = 1$ atm. The 1-hexanol molecules are highlighted by using white, red, and gray spheres for the hydroxyl hydrogen, oxygen, and CH_x groups, respectively, whereas the solvent molecules are shown in stick representation.

The goal of the present work is to calculate the vibrational absorption spectra for dilute solutions of 1-hexanol in *n*-hexane using an ensemble of aggregates that represents the distribution of aggregates obtained from the previous large-scale MC simulations. This ensemble of aggregates is then used as input for static electronic structure calculations and first-principles molecular dynamics simulations to calculate the vibrational absorption spectra for specific aggregates. With the aggregate distributions known it is then possible to determine contributions to the vibrational absorption spectra of the macroscopic solution weighted as a function of aggregate size and architecture. This route is preferable to direct molecular dynamics simulations or electronic structure calculations for the following reasons: (i) the long lifetime of these hydrogen-bonded aggregates and the low concentration of these solutions are far beyond what would be accessible to first-principles molecular dynamics approaches and (ii) a correct estimation of the entropic contribution to the Gibbs free energy of aggregate formation would be rather difficult for static electronic structure calculations.[14]

II. Computational Details

The ensemble of hydrogen-bonded 1-hexanol aggregates of sizes 1−5 was taken from a large-scale MC simulation[18] of a 3% solution of 1-hexanol in *n*-hexane at $T = 298$ K and $p = 1$ atm using a constrained random selection procedure to yield a good representation

(12) Provencal, R. A.; Paul, J. B.; Chapo, C.; Casaes, R. N.; Saykally, R. J.; Tschumper, G. S.; Schaefer, H. F., III. *J. Chem. Phys.* **1999**, *110*, 4258.
(13) Provencal, R. A.; Casaes, R. N.; Roth, K.; Paul, J. B.; Chapo, C.; Saykally, R. J.; Tschumper, G. S.; Schaefer, H. F., III. *J. Phys. Chem. A* **2000**, *104*, 1423.
(14) Sum, A. K.; Sandler, S. I. *J. Phys. Chem. A* **2000**, *104*, 1121.
(15) Mandado, M.; Grana, A. M.; Mosquera, R. A. *Chem. Phys. Lett.* **2003**, *381*, 22.
(16) Huisken, F.; Kulcke, A.; Laush, C.; Lisy, J. M. *J. Chem. Phys.* **1991**, *95*, 3924.
(17) Guedes, R. C.; do Couto, P. C.; Costa Cabral, B. J. *J. Chem. Phys.* **2003**, *118*, 1272.
(18) Stubbs, J. M.; Siepmann, J. I. *J. Phys. Chem. B* **2002**, *106*, 3968.
(19) Siepmann, J. I.; McDonald, I. R. *Mol. Phys.* **1992**, *75*, 255.
(20) Martin, M. G.; Siepmann, J. I. *J. Phys. Chem. B* **1998**, *102*, 2569.
(21) Chen, B.; Potoff, J. J.; Siepmann, J. I. *J. Phys. Chem. B* **2001**, *105*, 3093.

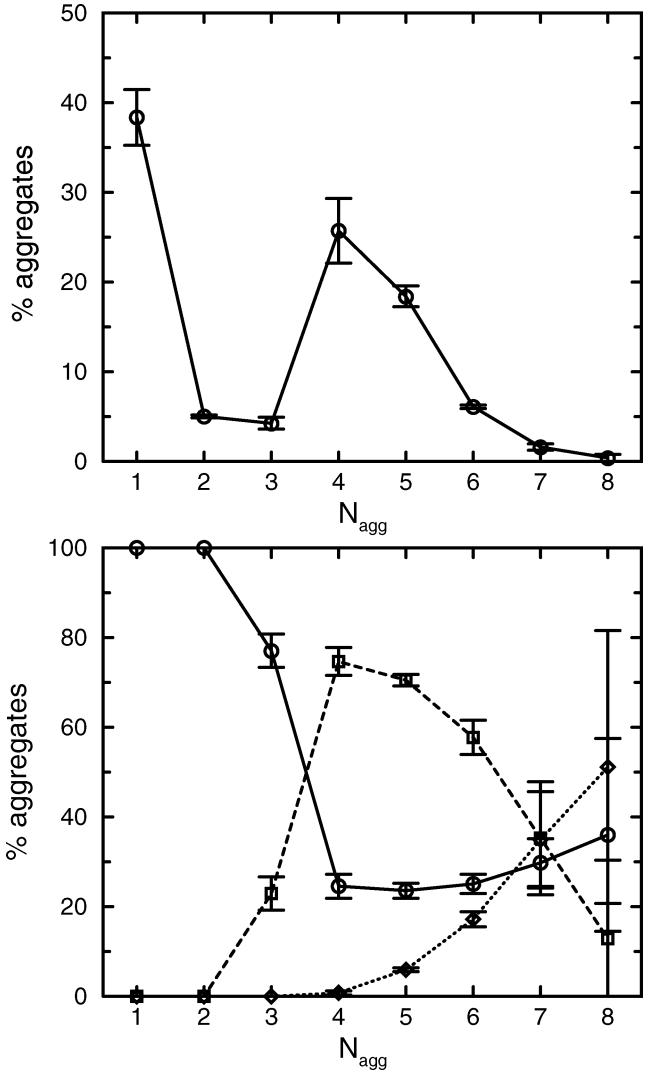

Figure 2. Distributions over aggregates sizes (top) and architectures for a given size (bottom) of 1-hexanol aggregates observed in the large-scale Monte Carlo simulation ($x_{hexanol} = 0.03$; $T = 298$ K; $p = 1$ atm).[18] The specific criteria used to define a hydrogen bond are described in the text.[22] ○, □, and ◇ in bottom panel denote linear, cyclic, and branched architectures, respectively. The lines are only drawn for guidance.

of the different sizes and architectures. To sort 1-hexanol aggregates by size and architecture, the following criteria were used to define a hydrogen bond: $r_{OO} \leq 3.3$ Å, $r_{OH} \leq 2.5$ Å, $\cos\theta_{OH\cdots OL} \leq -0.1$, and $u_{head} \leq -13$ kJ/mol, where r_{OO}, r_{OH}, $\cos\theta_{OH\cdots OL}$, and u_{head} are the oxygen−oxygen distance, the oxygen−hydrogen distance, the angle between the OH bond vector on the donating molecule and the oxygen lone pair vector on the accepting molecule, and the potential energy between the two $-CH_2OH$ headgroups, respectively[18,22]

Static electronic structure calculations were then carried out on 400 monomeric and 32 dimeric conformationally distinct 1-hexanol aggregates at the Hartree−Fock level with MIDI!-6D basis set[23] using an implicit representation of the *n*-hexane solvent via solvation model 5.42[24] as implemented in module MN-GSM[25] of Gaussian 98.[26] The clusters were first optimized to a local minimum in the potential energy surface, and thereafter a vibrational frequency analysis for the harmonic normal modes was performed. The calculated frequencies were scaled by a factor of 0.93 to bring the monomeric frequency into agreement with the experimental result for comparison with the subsequent methodologies employed. This value falls in the range of scaling factors that has been previously found to improve Hartree−Fock frequency results for different basis sets.[27] The subsequent spectra were averaged together for each size to capture the conformational broadening of peaks.

For the first-principles and classical molecular dynamics simulations, the ensemble of aggregates was prepared using the following procedure. An initial structure was generated by taking the 1-hexanol molecules of a given aggregate of size N_{agg} together with the N_{sol} closest solvent molecules determined from center-of-mass distances and constrained to yield a total of 10 molecules, that is, $N_{sol} = 10 - N_{agg}$. A fixed total number of molecules is preferable to using an unconstrained distance criterion because it minimizes systematic differences between calculations for aggregates of varying size. This 10-molecule system was then immersed in its own replicas using periodic boundary conditions for a cubic box with a length that resulted in a specific density about 10% lower than that of the large-scale MC simulation of the 1000-molecule system. After a brief equilibration period at constant volume, the 10-molecule system was further relaxed using a MC simulation in the isobaric−isothermal ensemble with an imposed external pressure of 1 atm and a temperature of 298 K. Throughout these simulations the TraPPE-UA force field[20,21] was used and the motion of the 1-hexanol molecules was restricted to coupled−decoupled configurational-bias Monte Carlo moves[28,29] of only the alkyl tails to preserve the aggregate architecture. At the end of these MC simulations, the positions of the hydrogen atoms belonging to the nonpolar methylene and methyl groups were determined using geometric considerations.[30]

Car−Parrinello molecular dynamics simulations[31] using the program CPMD[32] were carried out in a periodically replicated simulation cell using the Becke−Lee−Yang−Parr exchange and correlation energy functionals[33] in conjunction with Troullier−Martins norm-conserving pseudopotentials[34] and a plane wave basis set with a cutoff at the Γ-point of 85 Ry. To use a larger time step of 0.121 fs, the deuterium mass was used for the polar and nonpolar hydrogens and the fictitious electron mass employed was set to 700 au (appropriate for adiabatic sampling during the relatively short trajectories at ambient conditions[35]). An ionic kinetic temperature of 300 K was established via Nosé−Hoover chain thermostating of the electronic and nuclear degrees of freedom[36,37]

(22) The small differences between the values given here and those in ref 18 are due to a modification of the hydrogen-bonding criteria to better account for somewhat strained cyclic aggregates that were sometimes counted as multiple smaller aggregates in the earlier work.

(23) Easton, R. E.; Giesen, D. J.; Welch, A.; Cramer, C. J.; Truhlar, D. G. *Theor. Chim. Acta* **1996**, *93*, 281.
(24) (a) Li, J.; Hawkins, G. D.; Cramer, C. J.; Truhlar, D. G. *Chem. Phys. Lett.* **1998**, *288*, 293. (b) Zhu, T.; Li, J.; Hawkins, G. D.; Cramer, C. J.; Truhlar, D. G. *J. Chem. Phys.* **1998**, *109*, 9117.
(25) Xidos, J. D.; Li, J.; Thompson, J. D.; Hawkins, G. D.; Winget, P. D.; Zhu, T.; Rinaldi, D.; Liotard, D. A.; Cramer, C. J.; Truhlar, D. G.; Frisch, M. J. *MN-GSM*, version 1.6; University of Minnesota: Minneapolis, MN, 2001.
(26) Frisch, M. J.; Trucks, G. W.; Schlegel, H. B.; Scuseria, G. E.; Robb, M. A.; Cheeseman, J. R.; Zakrzewski, V. G.; Montgomery, J. A., Jr.; Stratmann, R. E.; Burant, J. C.; Dapprich, S.; Millam, J. M.; Daniels, A. D.; Kudin, K. N.; Strain, M. C.; Farkas, O.; Tomasi, J.; Barone, V.; Cossi, M.; Cammi, R.; Mennucci, B.; Pomelli, C.; Adamo, C.; Clifford, S.; Ochterski, J.; Petersson, G. A.; Ayala, P. Y.; Cui, Q.; Morokuma, K.; Malick, D. K.; Rabuck, A. D.; Raghavachari, K.; Foresman, J. B.; Cioslowski, J.; Ortiz, J. V.; Stefanov, B. B.; Liu, G.; Liashenko, A.; Piskorz, P.; Komaromi, I.; Gomperts, R.; Martin, R. L.; Fox, D. J.; Keith, T.; Al-Laham, M. A.; Peng, C. Y.; Nanayakkara, A.; Gonzalez, C.; Challacombe, M.; Gill, P. M. W.; Johnson, B. G.; Chen, W.; Wong, M. W.; Andres, J. L.; Head-Gordon, M.; Replogle, E. S.; Pople, J. A. *Gaussian 98*, revision A.9; Gaussian, Inc.: Pittsburgh, PA, 1998.
(27) Scott, A. P.; Radom, L. *J. Phys. Chem.* **1996**, *100*, 16502.
(28) Siepmann, J. I.; Frenkel, D. *Mol. Phys.* **1992**, *75*, 59.
(29) Martin, M. G.; Siepmann, J. I. *J. Phys. Chem. B* **1999**, *103*, 4508.
(30) Chen, B.; Siepmann, J. I. *J. Phys. Chem. B* **1999**, *103*, 5370.
(31) (a) Car, R.; Parrinello, M. *Phys. Rev. Lett.* **1985**, *55*, 2471. (b) Marx, D.; Hutter, J. In *Modern Methods and Algorithms of Quantum Chemistry*; Grotendorst, J., Ed.; NIC: Jülich, Germany, 2000; pp 301−449. See the Ab Initio Molecular Dynamics: Theory and Implementation Web site. www.theochem.ruhr-uni-bochum.de/go/cprev.html.
(32) CPMD, version 3.7; IBM Corp., MPI Stuttgart, 1990−2003; www.cpmd.org.
(33) (a) Becke, A. D. *Phys. Rev. A* **1988**, *38*, 3098. (b) Lee, C.; Yang, W.; Parr, R. C. *Phys. Rev. B* **1988**, *37*, 785.
(34) Troullier, N.; Martins, J. *Phys. Rev. B* **1991**, *43*, 1993.
(35) Kuo, I.-F. W.; Mundy, C. J.; McGrath, M. J.; Siepmann, J. I.; VandeVondele, J.; Sprik, M.; Hutter, J.; Chen, B.; Klein, M. L.; Mohamed, F.; Krack, M.; Parrinello, M. *J. Phys. Chem. B* **2004**, *108*, 12990.

throughout the equilibration period, which was turned off before the production periods that used microcanonical dynamics. The equilibration periods consisted of about 0.5 ps, and production runs ranging from 5 ps for the dimer to 11 ps for the larger aggregates were saved for subsequent analysis. It should be noted that even over the relatively short time span of these simulations, some of the aggregates undergo minor structural fluctuations and, for example, using a rather strict hydrogen-bond criterion (see above) a cyclic tetramer was observed to briefly undergo a transition to linear hydrogen-bond pattern (i.e., one of the hydrogen bonds weakened but the overall structure did not change to a more linear structure) before returning back to its complete cyclic hydrogen-bond pattern. For these cases, special care was taken that the analysis of the vibrational motion for a specific aggregate architecture was limited to the corresponding part of the simulation.

Classical dynamics simulations were carried out for the OPLS-AA force field[38] to assess whether a typical molecular mechanics force field using harmonic bond stretching potentials would be sufficient to yield accurate spectral shifts for hydrogen-bonded aggregates. The classical simulations were carried out using the Tinker program.[39] In this case, a 100-ps equilibration period using a Berendsen thermostat[40] was followed by a microcanonical trajectory of the same duration.

For a given Car−Parrinello or classical molecular dynamics simulation, the vibrational absorption spectrum was determined using the velocity autocorrelation function of the hydroxyl hydrogen that was transformed into the frequency domain using the regularized resolvent transform[41] to determine the power spectrum, which allowed for more precise peak shapes and a higher resolution of about 1 cm^{-1} than the equivalent discrete Fourier transform. Furthermore, the frequencies for the CPMD simulations were corrected through multiplication by $\sqrt{2}$ to approximately account for the difference of the hydrogen and deuterium masses. No further scaling was required to bring the monomeric peak for the CPMD simulations into agreement with experiment due to a fortuitous cancellation of errors; the first being due to inaccuracies of the BLYP functional and the second being due to a slowing of the vibrational dynamics caused by the fictitious electron mass.[42] For the classical molecular dynamics simulations, all frequencies were scaled by 0.96 to bring the monomer absorption peak into agreement with experiment.

III. Results

Figure 3 shows a comparison of average vibrational spectra for isolated 1-hexanol molecules and dimeric aggregates computed by the static quantum chemical approach to the experimental data for a dilute solution of 1-hexanol in *n*-hexane.[4] It is clearly evident that the computed spectra for both monomer and dimer show a peak at 3650 cm^{-1}, and this peak is present for all 32 dimer configuration studies here. Furthermore, the absorption intensities per aggregate (i.e., not weighted by their occurrence in the large-scale MC simulation) are very similar. Thus, it appears that indeed one hydroxyl group in every dimer contributes to the nondonating hydroxyl peak which agrees with the result of the large-scale MC simulations (see Figure 2) that all dimers are linear and are bound by a single hydrogen bond. Clearly, the contribution of dimers needs to be removed from the peak arising from nondonating hydroxyl group when one wants to determine the true number of isolated molecules (monomers).

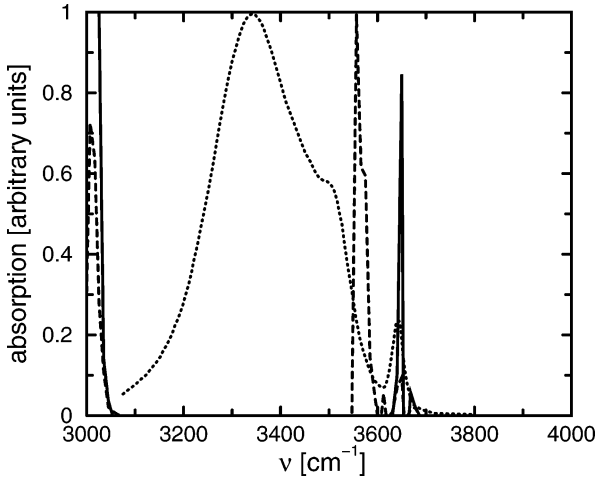

Figure 3. Comparison of the vibrational spectra computed using static electronic structure calculations at the HF/MIDI!-6D level using an implicit solvation model with the experimental data (dotted line) for a dilute solution of 1-hexanol in *n*-hexane.[4] The solid and dashed lines show the computed spectra for monomeric and dimeric aggregates averaged over different starting structures and weighted to reflect their relative population in solution.

In addition to the nondonating peak, the computed spectra for the dimers contain another peak at 3560 cm^{-1} arising from the donating hydroxyl group. The frequency shift of 90 cm^{-1} is somewhat smaller than the experimental data for the dimer-like frequency shift of 107 cm^{-1} for methanol in the gas phase[16] and 140 cm^{-1} for methanol in a solid argon matrix.[7] The position of this donating peak for the dimer is also consistent with the shoulder at 3510 cm^{-1} observed in the experimental spectrum for 1-hexanol in *n*-hexane.[4] However, it is clearly smaller in magnitude than the experimental shift found for the main peak position arising from solvated hydrogen-bonded aggregates. The computed spectrum for the dimer shows evidence of conformational broadening, that is, the repetition of the calculation for different initial molecular conformations leads to different local minima on the potential surface that have slightly different spectroscopic characteristics. However, no attempt is made here to estimate the effects of finite temperature on the distribution of aggregate conformations and their spectra. The static electronic structure calculations were not extended to larger aggregate sizes due to the slow convergence to minima in the potential energy landscape caused by the flexible tails of the hexanol molecules.

The application of the CPMD approach to the 1-hexanol/*n*-hexane solution allows one to treat the intra- and intermolecular interactions quantum mechanically while maintaining a finite temperature and sampling local rearrangements of the aggregate structures through classical motion of the solute and solvent molecules. The calculated spectra from CPMD velocity autocorrelation functions of the hydroxyl hydrogen atom include not only the bond stretching mode but also all other types of motion (e.g., bond bending, libration, and translation) that appear at lower frequencies. As an illustrative example, the complete spectrum for a 1-hexanol monomer (solvated by 9 *n*-hexane molecules) is shown in Figure 4. It should be emphasized here that, due to the analysis method based on the velocity autocorrelation function, the power spectra presented here lack informa-

(36) Martyna, G. J.; Tuckerman, M. E.; Klein, M. L. *J. Chem. Phys.* **1992**, *97*, 2635.
(37) Tuckerman, M. E.; Parrinello, M. *J. Chem. Phys.* **1994**, *101*, 1302.
(38) Jorgensen, W. L.; Maxwell, D. S.; Tirado-Rives, J. *J. Am. Chem. Soc.* **1996**, *118*, 11225.
(39) (a) Ren, P.; Ponder, J. W. *J. Phys. Chem. B* **2003**, *107*, 5933. (b) See the Tinker Home Page. http://dasher.wustl.edu/tinker.
(40) Berendsen, H. J. C.; Postma, J. P. M.; van Gunsteren, W. F.; DiNola, A.; Hauk, J. R. *J. Chem. Phys.* **1984**, *81*, 3684.
(41) Chen, J.; Shaka, A. J.; Mandelshtam, V. A. *J. Magn. Reson.* **2000**, *147*, 129.
(42) Tangney, P.; Scandolo, S. *J. Chem. Phys.* **2002**, *116*, 14.

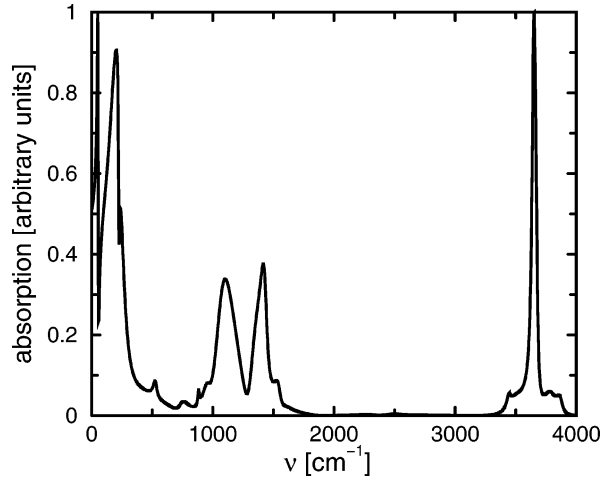

Figure 4. Vibrational density of states of a solvated 1-hexanol monomer obtained through the regularized resolvent transform of the velocity autocorrelation function from a CPMD simulation.

tion on the transition dipole moment of the vibrations. Therefore, peak heights do not reflect actual IR absorption intensities.

The largest density of states in the CPMD dimer power spectrum occurs at 3630 cm^{-1}, near the monomeric value, and a much smaller second peak is centered at 3540 cm^{-1} (see Figure 5a). As expected, further analysis shows that the former peak is associated with the vibration of the nondonating hydroxyl group, while the latter peak arises from the donating group. The frequency shift of about 100 cm^{-1} going from monomer (see Figure 4) to dimer is in excellent agreement with the shift computed from the static electronic structure calculations. Additionally, the absolute positions of both peaks are in good agreement with the experimental monomer-like peak and the shoulder between monomer and bulk hydrogen-bonded values. In contrast to the static approach, thermal broadening results in a substantial red-shifted tail for the donating hydroxyl group. However, the tail does not extend down to the location of the main peak for hydrogen-bonded aggregates found in the experimental study.[4]

As depicted in Figure 5b, the vibrational density of states for a single trimeric aggregate with linear architecture (i.e., two hydrogen bonds) shows two large peaks located at 3640 and 3520 cm^{-1} and a substantially smaller peak shifted further to lower frequency at 3430 cm^{-1}. Evidently, the high-frequency peak arises from the terminal hydroxyl group of the linear trimer that does not act as a hydrogen-bond donor and therefore appears together with the absorption for isolated alcohols. A trimer is also the smallest aggregate size that can show the effects of hydrogen-bond cooperativity, and indeed, the split of the hydrogen-bonded region into two peaks indicates two donating hydroxyl groups in distinct environments. Further examination of the simulation results into contributions of individual hydroxyl hydrogens reveals that the hydrogen of the alcohol located in the middle of the linear trimer (i.e., belonging to a hydroxyl group that accepts a hydrogen bond and donates to a terminal hydroxyl group) only contributes to the middle spectral peak at 3520 cm^{-1}, close to the value of 3540 cm^{-1} associated with the donating hydroxyl group found for the dimeric aggregate. Finally, the donating hydroxyl group at the other end of the trimeric aggregate can be considered to be making a hydrogen bond to an acceptor hydroxyl group that is also a donor of another hydrogen bond. This situation is known to enhance the stability of the former hydrogen bond due to longer range interactions such as favorable dipole−dipole interactions as well as the increased polarization of the hydroxyl group that acts as both acceptor and donor.[4,14,18] It is this hydroxyl group at the terminal end that shows a minor peak with a red-shifted absorption at 3430 cm^{-1} though it mainly contributes to the central peak most likely due to the multiple conformations adopted by the aggregate throughout the simulation. This is consistent with an earlier computational study of methanol clusters of different architectures where frequency shifts of −200 and −260 cm^{-1} were observed for the central and terminal donating hydroxyl groups, respectively.[10] It should be noted here that this pattern of dimer-like and cooperative (or polymer-like) hydrogen bonds is different from the picture assumed by Gupta and Brinkley (see Figure 4 of ref 4) for the justification of the hydrogen-bond theory with cooperativity where the hydrogen bond formed by the donating terminal hydroxyl group was termed as dimer-like, whereas the hydrogen bond formed by the next-to-last hydroxyl group with the nondonating terminus was termed polymer-like.

The power spectra for three cyclic and one linear tetrameric aggregates are shown in Figure 5c. Although individual aggregates produce substantially different spectra (see below), the main absorption for the tetrameric aggregates is a broad peak centered at ∼3320 cm^{-1}. For the linear tetramer, the nondonating terminal hydroxyl group contributes to the monomeric-like absorption peak and hydrogen-bond cooperativity is manifested in the split of the hydrogen-bonded peak. The spectra of the three cyclic aggregates show a substantial diversity with different overall peak shapes and different average shifts reflecting the different structural environments for the various hydroxyl groups contributing to the overall absorption. Most importantly, none of the cyclic tetramers show any significant vibrational motion at the high frequency of about 3640 cm^{-1} associated with a nondonating hydroxyl group (i.e., the cyclic structures involve solely donating hydroxyl groups). Furthermore, only two of the cyclic tetramers show a very small peak for motion in the dimer-like range close to 3540 cm^{-1} (i.e., strained conformations that do not allow a donating hydroxyl group to feel the cooperative effect are rarely encountered). This is in contrast to the finding for the linear trimer where the terminal donating hydroxyl group yields a significant contribution to the dimer-like vibrational region.

The large-scale MC simulations showed that pentameric aggregates possess more diverse architectures with branched aggregates (one alcohol acting as double acceptor and single donor) in addition to linear and cyclic architectures (see Figure 2). No attempt was made to distinguish between branched pentameric aggregates that have architectures with bonding patterns resembling either 2-methyl butane or methyl cyclobutane. Overall, the four pentameric aggregates investigated using the CPMD approach have the largest vibrational density in the region from 3340 to 3410 cm^{-1} (see Figure 5d). As should be expected, both the linear and branched architectures yield significant contributions to the monomer-like and dimer-like peaks. Judging from the single branched architecture investigated here, it does not appear that the shifts of hydroxyl groups donating a hydrogen bond to the double acceptor/single donor branch point fall outside the usual range of cooperative

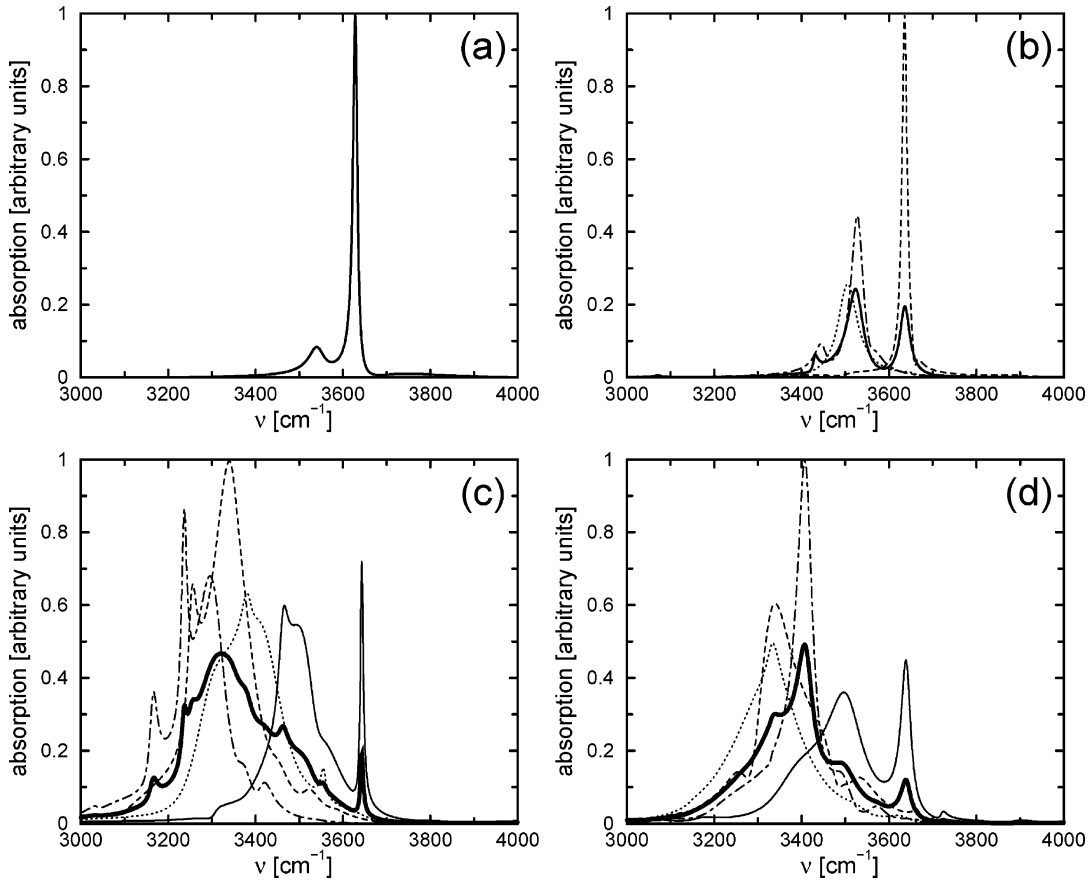

Figure 5. Vibrational density of states for different aggregate sizes and architectures obtained from separate CPMD simulations. (a) Linear dimer. (b) Linear trimer. The solid, dashed, dotted, and dash−dotted lines denote the average power spectrum for the trimer and the contributions of the nondonating terminal hydroxyl group, the middle hydroxyl group, and the donating terminal hydroxyl group, respectively. (c) Tetramers. The thin solid, dashed, dotted, and dash−dotted lines denote the spectra of a linear tetramer and three different cyclic tetramers, respectively. The thick solid line shows the weighted average (according to the distribution over aggregate architectures) for tetrameric aggregates. (d) Pentamers. The thin solid, dashed, dotted, and dash−dotted lines denote the spectra of a linear, a branched, and two different cyclic pentamers, respectively. The thick solid line shows the weighted average (according to the distribution over aggregate architectures) for pentameric aggregates.

(polymer-like) hydrogen bonds found in linear and cyclic aggregates. As also observed for tetramers, the cyclic pentamers do not make a significant contribution to the dimer-like region of the spectrum (i.e., hydrogen-bond cooperativity is maintained most of the time). It is not clear whether the observation that the main peak for the cyclic pentamers is slightly less red-shifted than that for the cyclic tetramers is significant or within the noise of the small number of simulations carried out here. A possible source of error might be that the 10-molecule system size used here imposes some strain on the larger pentameric aggregates.

As mentioned earlier, all cluster sizes including the larger tetramers and pentamers were observed to contribute substantially to the monomer-like and dimer-like peaks in the power spectrum. To emphasize this point, Figure 6 shows the vibrational density of states computed for specific types of hydrogen bonds. These power spectra were obtained as follows. For all trimers, tetramers, and pentamers, the hydrogen-bonding pattern was analyzed throughout the course of the CPMD simulations using the hydrogen-bond criteria taken from the large-scale MC simulations (see section II). Subsequently, for each hydroxyl group the fraction of time was determined for each of the three cases: (i) acceptor-only (monomer-like), (ii) acceptor and donor, donating to an acceptor-only hydroxyl group (dimer-like), or (iii) acceptor and donor, donating to an acceptor−donor hydroxyl group (polymer-like). The hydroxyl groups were then grouped together according to which case they had spent the majority of the simulation time, and the power spectrum of each hydroxyl group was computed from its individual autocorrelation function using only the time segment-(s) spent in that particular case. Finally, to compare spectra from different aggregate sizes and/or architectures, each spectrum was weighted according to the probability of appearance of that aggregate and architecture (see Figure 2).

The ensemble-averaged power spectrum for the CPMD simulations was calculated by averaging over the different aggregate sizes and architectures in a weighted fashion according to the distribution found in the large-scale MC simulation[18] (see Figure 2) using the assumptions that the contributions from the different hexameric architectures are equivalent to their pentameric counterparts and that aggregate sizes with more than six alcohols can be neglected. As seen in Figure 7, the ensemble-averaged power spectrum with its monomer-like, dimer-like, and cooperative (polymer-like) hydrogen-bonded absorption features is in very satisfactory agreement with the experimental data.[4] As noted by one of the reviewers, the difference in the relative intensities of the monomer-like and polymer-like peaks may be partially attributed to an increase of the measured IR intensity for hydrogen-bonded hydroxyl groups due to charge transfer upon hydrogen-bond formation, which would not be

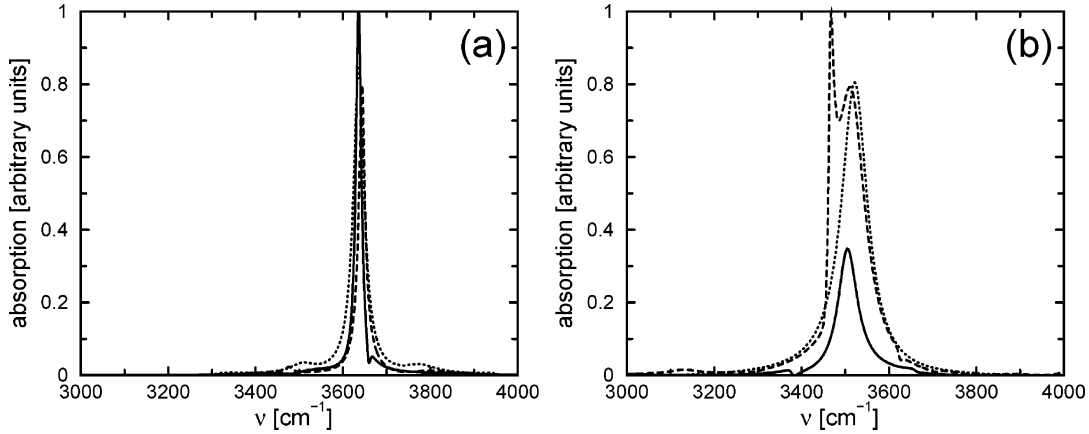

Figure 6. Vibrational density of states for hydroxyl groups participating in the formation of (a) monomer-like and (b) dimer-like hydrogen bonds. The solid, dashed, and dotted lines denote the weighted averages (according to the distribution over aggregate architectures) for trimeric, tetrameric, and pentameric aggregates, respectively.

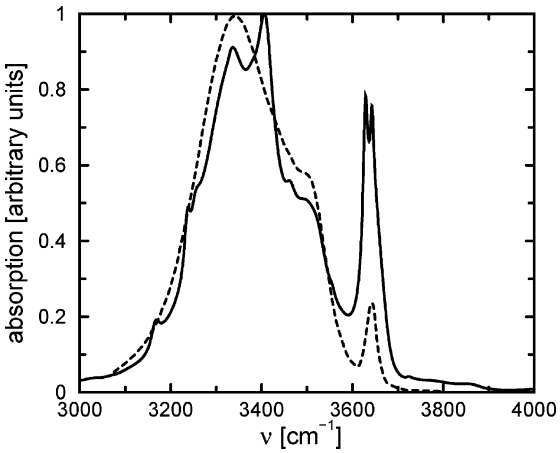

Figure 7. Ensemble-averaged power spectrum computed from the CPMD simulations (solid line) plotted along with experimental results (dashed line).[4]

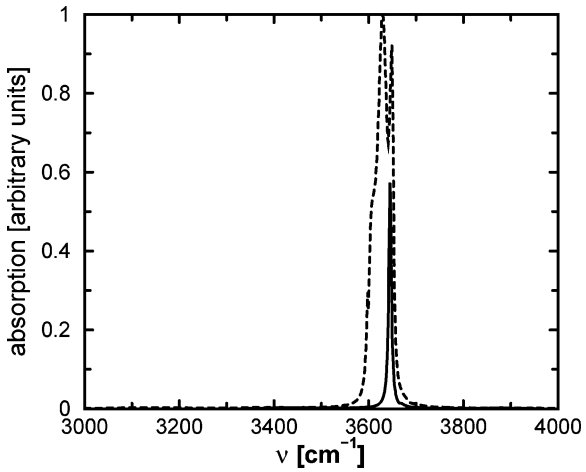

Figure 8. Vibrational densities of state for monomeric (solid line) and tetrameric (dashed line) aggregates computed from classical molecular dynamics simulations with the OPLS-AA force field.

reflected in the power spectrum computed from the velocity autocorrelation function. Thus, these CPMD simulations strongly support the notion that the aggregate sizes and architectures present in finite-temperature dilute solutions of alcohols in nonpolar solvents are substantially more diverse than a simple equilibrium involving solely monomers and cyclic tetramers.

Finally, for comparison classical molecular dynamics simulations were also carried out for a monomer and a tetramer using the empirical OPLS-AA force field (see Figure 8). The power spectrum for the tetramer shows a distinct peak that coincides with the monomer peak, another peak that is red-shifted by about 20 cm^{-1}, and a weak shoulder with a shift of about 40 cm^{-1}. During the course of the much longer simulation for the OPLS-AA force field, significant conformational fluctuations were encountered for the tetramer (although it remains stable over the entire period), which makes it impossible to assign the two lower frequency peaks to specific architectures or molecules. However, it is clearly evident that an empirical nonpolarizable force field with a harmonic vibrational potential is not able to reproduce even qualitatively the spectral features of hydrogen-bonded aggregates in solution.

IV. Conclusions

A multiscale modeling approach consisting of static electronic structure calculations with an implicit solvent (MN-GSM) and CPMD simulations with explicit solvent molecules for specific aggregates selected from a large-scale Monte Carlo simulation was applied to elucidate the vibrational spectrum of dilute solutions of 1-hexanol in *n*-hexane. In agreement with the experimental data, the computed spectra show three important features: a relative narrow "monomer-like" absorption peak at about 3650 cm^{-1}, a very broad "polymer-like" absorption peak red-shifted by about 300 cm^{-1} with a "dimer-like" shoulder that is red-shifted by about 150 cm^{-1}. The MN-GSM and CPMD computations demonstrate that the dangling hydrogen bonds found in all dimers and larger aggregates with linear or branched architecture absorb at the "monomer-like" frequency. The "dimer-like" shoulder arises mainly from noncooperative hydrogen bonds formed by the next-to-last 1-hexanol molecule with an acceptor-only chain terminus of linear and branched aggregates consisting of 4−6 1-hexanol molecules, whereas the absorption of the hydroxyl group donating the single hydrogen bond in "true" dimers is red-shifted to a smaller degree (only about 100 cm^{-1}) and does not contribute significantly to the overall absorption spectrum because of the relatively low abundance of dimeric aggregates. Cooperative hydrogen bonds found in all larger aggregates (trimers and beyond) contribute to the "polymer-like" absorption feature. In particular, cyclic

aggregates are found to absorb almost exclusively in the "polymer-like" region.

The CPMD simulations point to significantly different spectral features for aggregates of the same size but with different architecture (i.e., there is no simple way that would allow the deconvolution of experimental vibrational spectra to determine the contribution of specific aggregate sizes nor architectures). Furthermore, the inclusion of thermal effects appears to be imperative for the prediction of vibrational spectra in solution to account for thermal broadening and for the contribution of aggregate architectures that are not the lowest-energy structure for a given size (e.g., linear tetramers). Overall, the ensemble-averaged power spectrum computed from the CPMD simulations (with weights for specific aggregates sizes and architectures taken from the large-scale MC simulation) shows very satisfactory agreement with the experimental data. Thus, one needs to conclude that the distribution of alcohol aggregates in nonpolar solvents is more complex than the often assumed equilibrium of monomers and cyclic tetramers.

Acknowledgment. We thank Will Kuo and James Xidos for assistance setting up the CPMD and MN-GSM calculations as well as advice regarding spectra determination and the anonymous reviewers for helpful comments. Financial support from the National Science Foundation (CTS-0138393), a DAAD Fellowship, a Frieda Martha Kunze Fellowship, a University of Minnesota Doctoral Dissertation Fellowship, and the University Relations Program of Lawrence Livermore National Laboratory (DOE W-7405-End-48) is gratefully acknowledged. Part of the computer resources were provided by the Minnesota Supercomputing Institute.

JA044380Q